Review

Brownian motion in electrochemical nanodevices

K.J. Krause[1], K. Mathwig[2], B. Wolfrum[1,3], and S.G. Lemay[4,a]

[1] Institute of Bioelectronics (PGI-8/ICS-8) and JARA; Fundamentals of Future Information Technology, Forschungszentrum Jülich, 52425 Jülich, Germany
[2] Institute for Integrative Nanosciences, IFW Dresden, Helmholtzstr. 20, 01069 Dresden, Germany
[3] Institute of Physics, RWTH Aachen University, 52074 Aachen, Germany
[4] MESA+ Institute for Nanotechnology, University of Twente, PO Box 217, 7500 AE Enschede, The Netherlands

Abstract. Diffusion dominates mass transport in most electrochemical systems. In classical experimental systems on the micrometer scale or larger, this is adequately described at the mean-field level. However, nanoscale detection devices are being developed in which a handful or even single molecules can be detected. Brownian dynamics become manifest in these systems via the associated fluctuations in electrochemical signals. Here we describe the state of the art of these electrochemical nanodevices, paying particular attention to the role of Brownian dynamics and emphasizing areas in which theoretical understanding remains limited.

1 Introduction

Electrochemistry encompasses a wide range of concepts and experimental techniques dealing with the transfer of charge between electronic and ionic conductors. It finds widespread application in fields as diverse as energy storage, the semiconductor industry and bioanalytical technology. Broadly speaking, an electrochemical process can be broken down into two separate components, namely (1) a chemical reaction involving the transfer of electrons and (2) mass transport of the species involved in this reaction. Detailed understanding of the electron-transfer process necessarily involves a description at the molecular level, whereas mass transport is most commonly described at the mean-field level using formalisms such as the Nernst-Planck equation [1].

In recent years there have however been increasing efforts to miniaturize electrochemical measurement systems to the micro- or nanometer scale. This activity is driven both by attempts at exploring fundamental electrochemical processes on these length scales as well as the ambition to develop new types of miniaturized, chip-based analytical tools [2]. A side-effect of miniaturization is that the numbers of particles

[a] e-mail: s.g.lemay@utwente.nl

involved in a measurement can become sufficiently small that discreteness effects and departures from mean-field descriptions due to Brownian fluctuations can become experimentally significant. The extreme case is that of a single molecule diffusing in a nanoscale channel: experimental methods have now reached the point where electrical tracking of single molecules is becoming possible [3], necessitating the use of new theoretical frameworks to quantitatively describe mass transport.

The objective of the present article is to introduce nanoelectrochemical systems and their conceptual challenges in a way that is readily accessible to a non-electrochemistry audience. In particular, we eschew as much as possible all details that depend on specific chemical and/or material properties and focus instead on prototypical experimental systems that are more amenable to a general theoretical description. We assume that the reader has some general familiarity with mass transport and random-walk processes.

It should be noted that the field is still in its infancy. Only a handful of experimental groups have so far tackled the experimental systems described here, and, despite notable numerical studies, few purely theoretical works have directly addressed these experiments in a quantitative way. Indeed, we also point out several outstanding questions along the way; we hope in so doing to stimulate the theoretical reader in search of new problems of interest.

2 Electrochemistry

The term electrochemistry encompasses a vast number of physical and chemical phenomena. Many important systems – for example in the areas of energy conversion and electrodeposition – depend critically and intricately on material properties, making it impractical to discuss the field as a whole here. We therefore instead concentrate on a specific set of idealized conditions which are (mostly) independent of material-specific behavior and are thus particularly amenable to quantitative analysis. In terms of eventual applications, these prototypical scenarios are mostly representative of situations in which electrochemistry is used as an analytical method to quantify the contents of a solution. More specifically, we focus here on phenomena related to mass transport and that satisfy the following conditions:

– *Electron transfer occurs between an electrode and molecules in solution.* While many important electron transfer reactions take place between two or more molecules in solution, a scenario more typical of analytical applications is that the electrons hop between a solid-state electrode and molecules in a solution that is in direct contact with the electrode. The electrostatic potential of the electrode can be controlled externally, and the resulting flux of electrons is a current that can be measured to quantify the rate at which the reaction takes place. Unreacted molecules are named the substrate (not to be confused with solid-state physics usage of the term!) and reacted molecules are called the product of the reaction.
– *Diffusive mass transport is dominant.* The most common electrochemically detectable analytes are small molecules in a room-temperature solution. Their Brownian motion is usually the dominant contribution to mass transport on the micro- or nanoscale, in which case the average number density of particles, $n(r,t)$, is described by the diffusion equation, $\partial_t n(\mathbf{r}, t) = D\nabla^2 n(\mathbf{r}, t)$, where D is the diffusion coefficient.
– *Convection can be induced.* While many electrochemical measurements rely purely on diffusion, it is also possible (and often desirable) to induce convection (or, more precisely, advection in the case of a linear channel) by mechanically actuating the solution with velocity $v(\mathbf{r}, t)$.

– *Migration due to electric fields can be ignored.* Given the fact that electrochemistry is an electrically-driven phenomenon, it may at first seem counterintuitive to ignore electrostatics. However, electrochemical measurements are most commonly carried out under conditions in which a high concentration of inert ions (the so-called supporting electrolyte) is also present. As a result, the charge at electrodes is locally compensated by screening ions accumulating near the surface of the electrodes, and electromigration plays no role beyond a short distance from the electrodes. This is particularly true in biochemical applications since the high salt concentration of physiological solutions ($>0.1\,\mathrm{M}$ monovalent salt) means that electric fields are screened within a few nanometers from the surface of a charged object. Under these conditions, the fact that substrate and product molecules have different charges does not influence their behavior. Note that this assumption ceases to be true at very short time scales during transients, but we will not consider this more specialized topic here.

– *Electron transfer is automatic and instantaneous.* Electron transfer between a molecule and an electrode can only take place once the distance between them becomes so short (order $1\,\mathrm{nm}$) that electrons can tunnel between them. The hopping process is usually characterized by a rate constant that depends sensitively on parameters such as the distance to the electrode, the nature of the solvent, the internal dynamics of the molecule and the electrostatic potential applied to the electrode. For many commonly employed analyte molecules with fast electron-transfer rates, however, the rate can be made sufficiently high (mostly by increasing the electrostatic driving force) that it ceases to be a bottleneck in the total reaction rate compared to mass transport. In these cases it is expedient to treat the rate as infinite and to concentrate on the more critical mass transport processes. This is not to say that situations where electron transfer dynamics become relevant are uninteresting or unimportant, but rather that detailed studies of their effect on stochasticity at the nanoscale currently lie beyond the state of the art.

– *Substrates and products are soluble.* We will only consider systems in which all substrate and product molecules are soluble, thus explicitly excluding electroplating and corrosion processes. A class of prototypical systems satisfying this condition are so-called "outer sphere" reactions, in which both substrate and product molecules remain fully solvated while one or more electrons tunnel to or from the electrode. Most experiments on stochastic electrochemistry to date were performed with such outer-sphere systems, making this a good starting point for theoretical descriptions. For simplicity, we will assume here that the diffusion coefficient D of an outer-sphere species is independent of the charge state of the molecule (i.e., substrate and product have the same value of D).

We emphasize that the above represent highly idealized conditions under which to perform electrochemistry. Many important problems in the field, for example in the energy and complex fluid analysis sectors, depend on overcoming difficulties that were purposefully omitted in the above formulation. On the other hand, these idealized experimental conditions represent an ideal starting point for investigating the role of Brownian processes in electrochemistry, and more generally for quantitative studies of electrochemical processes on the nanoscale.

3 Single electrodes and shot noise

Consider a simple electrochemical system consisting of a suitably biased electrode of finite dimensions immersed in a solution containing an average number density n_0 of outer sphere, electrochemically active molecules. Substrate (s) molecules that diffuse to the surface of the electrode react by donating or receiving z_e electrons
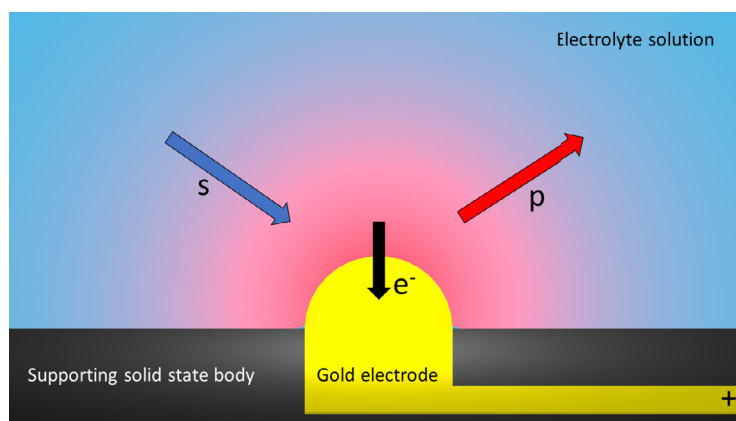
Fig. 1. Sketch of the diffusional mass transport to a hemispherical electrode. A redox-active substrate (s, blue) is converted at the electrode (yellow) to a product (p, red) leading to an effective net transport of substrate and product molecules to and from the electrode, respectively.

($z_e = 1$ being most typical), then diffuse away as product (p) molecules. Repeated collisions between a product molecule and the electrode do not lead to additional electron transfer since the molecule has already "switched" its charge state to that of a product. The average electrochemical current is thus simply proportional to the rate of collisions of substrate molecules with the electrode.

As a specific illustration, consider a simple hemispherical electrode of radius R emerging out of an insulating planar surface, as sketched in Fig. 1, subject to purely diffusional bulk mass transport. The number density of substrate molecules is subject to the diffusion equation with, as boundary conditions, $n_s(r \to \infty) = n_0$ (bulk conditions far from the electrode) and $n_s(R) = 0$ (substrate reacts at the surface of the electrode). The average number density of substrate molecules then exhibits a radially symmetric stationary solution to the diffusion equation, $n_s(r) = (1 - R/r)n_0$. The corresponding steady-state electrochemical current $\bar{i}$ is given by the diffuse flux at the electrode surface times the charge z_e transfered per collision,

$$\bar{i} = 2\pi z_e eDRn_0, \tag{1}$$

where $-e$ is the charge of the electron. More complex geometries lead to the same result within a multiplicative factor [4]. The corresponding density of product molecules also obeys the diffusion equation with boundary conditions $n_p(r \to \infty) = 0$ (no product in the bulk) and $\partial_r n_p(R, t) = -\partial_r n_s(R, t)$ (product molecules created at the electrode at the same rate as substrate molecules are being annihilated). The resulting product density is maximal at the surface of the electrode and decays with distance as $n_p(r) = (R/r)n_0$ under steady-state conditions.

Missing from the above description is the role of fluctuations associated with the discreteness of the individual electron-transfer events. This topic was studied by several authors from the 1970s onward with the aim of elucidating experimentally the microscopic electrochemical process [5–10]. Under the steady-state conditions sketched here, and under the simplifying assumption that the electron-transfer process takes place instantaneously at the electrode surface, the predicted current noise power spectrum is however simply predicted to be that of conventional shot noise, $S(f) = 2e\bar{i}$ [5,9,10]. No system-specific information can therefore be gleaned. Less idealized assumptions, for example taking into account a finite interaction time between molecule and electrode, does lead to more complex predicted spectra, but
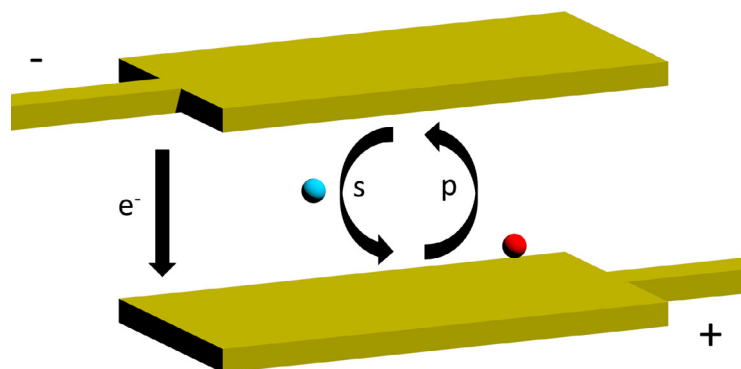
Fig. 2. Sketch of the redox cycling process at two individually biased electrodes. Upon reaction with the electrodes, molecules change their charge state leading to a transfer of electrons from the top to the bottom electrode with each cycle.

only at correspondingly fast time scales. Extracting high-frequency noise spectra is particularly challenging due to the relatively low signal levels involved, the co-occurence of thermal noise, and the fact that the response of the solution must be taken into account in analyzing experimental results, at least at the level of lumped circuit elements representing the screening ions at the electrode surface (a non-linear capacitance) and the solution resistance [5,8–10]. These limitations are in principle mitigated at nanoscale electrodes, which exhibit fast RC relaxation times and lower current levels, the latter corresponding to larger shot noise amplitudes as a fraction of the total current. So far this type of detailed noise study has however not been attempted at nanoelectrodes or, when it was, appeared to be dominated by slow relaxation processes associated with the electrode rather than Brownian motion [11].

4 Amplifying the role of discrete molecules: Redox cycling

The main experimental challenge in investigating electrochemistry at the level where Brownian fluctuations become relevant is ultimately the difficulty of measuring the low signal levels associated with individual electron-transfer events. One way to overcome this in experiments is to boost the amount of charge being transfered to an electrode by each molecule, such that the signature of each molecule becomes more experimentally accessible and therefore smaller numbers of molecules can be probed. The main method for achieving such amplification is so-called redox cycling, as illustrated in Fig. 2. Two electrodes are employed, the first electrode being biased such that substrate molecules are turned into products and the second electrode turning these product molecules back into substrates so that the cycle can be repeated again. If the two electrodes are located in close proximity, Brownian motion of each molecule between the two electrodes leads to repeated back-and-forth conversion between the two charge states, each cycle leading to z_e electrons being transfered from one electrode to the other.

Several realizations of this experiment have been achieved. These include inter-digitated arrays, which employ interlocking comb-shaped electrodes [12,13]; ring-disk electrodes, in which a central disk-shaped electrode is surrounded by a ring-shaped "collector" electrode [14–16]; and thin-layer cells, consisting of two planar electrodes separated by a thin layer of fluid [2,17]. The latter geometry lends itself particularly well to experiments on small numbers of molecules as it (at least temporarily)
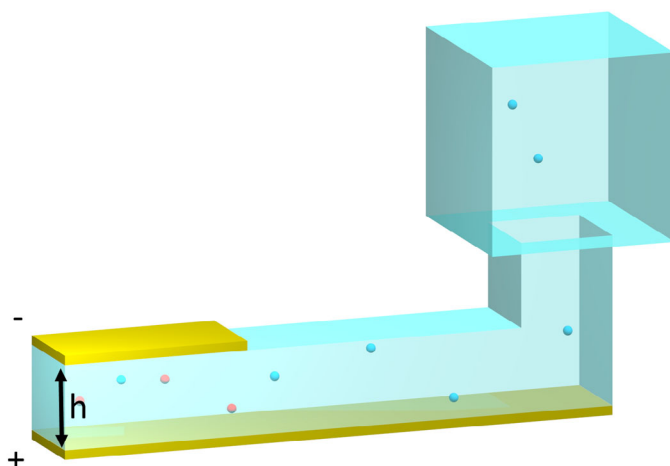
Fig. 3. Sketch of a nanofluidic redox cycling sensor design. Electrodes are integrated into the top and bottom of a nanochannel, which is connected to a bulk reservoir.

isolates the molecules located between the electrodes from external bulk solution, allowing measurements on well-defined numbers of molecules.

The first such experiments at the nanoscale were based on metal tips shrouded in wax that were pushed against a surface to trap a small volume of solution containing target molecules [18]. A later, more sophisticated variant employed recessed disk electrodes shrouded in glass and immersed in liquid mercury to trap a small volume of solution between two conducting surfaces [19]. Finally, we have developed microfabricated nanochannels whose floor and roof consist of separately addressable electrodes (see sketch in Fig. 3). In each of these thin-layer cell cases, net diffusion between the electrodes is essentially one-dimensional and leads to linear concentration profiles, $n_s(z) = (z/h)n_0$ and $n_p(z) = (1 - z/h)n_0$ [20,21]. Here h is the distance between the planar electrodes and z is the position along the normal direction. The corresponding electrochemical current is

$$\bar{i} = \frac{z_e e D A n_0}{h} = \bar{N}\frac{z_e e D}{h^2},\tag{2}$$

where A is the area of overlap of the electrodes and $\bar{N} = hAn_0$ is the number of analyte molecules in the detection volume. The second form emphasizes that each molecule in the detection region contributes a steady-state current $z_e e D/h^2$, the total current being thus proportional to the number of molecules. For $h = 100$ nm and typical small analyte molecules in water this current per molecule is of order $10\,\mathrm{fA}$, which is (just) experimentally accessible; smaller spacing translates in principle into higher signals still. Furthermore, because of the small detection volume, concentrations corresponding to order one molecule in the detection volume become experimentally accessible.

5 Equilibrium number fluctuations

5.1 Theory

In the nanofluidic thin-layer cell approach, the electrodes are imbedded in a channel that connects to an external bulk reservoir of solution. In this case N is not fixed and

can instead vary with time as individual molecules undergo Brownian motion in and out of the detection region. In realizations of these devices to date, the typical spacing between the electrodes is in the range 40–60 nm while the length of the detection region is of the order 10–100 μm. As the diffusion time scales quadratically with the distance, there is thus a separation of time scales for diffusion between the electrodes (z direction) and longitudinally along the channel (x direction) of order 10^5–10^6, z-motion taking place on the μs scale and x-motion on the scale of seconds. This means that measurements that average the electrochemical current on a time scale of order ms or longer tend to smear out fluctuations resulting from the shuttling dynamics but can still resolve the slow variations in N. That is, to a first approximation the measured current is simply $i(t) = N(t)(z_e e D/h^2)$. Measurements of the low-frequency noise in such a system indeed show that the noise amplitude scales as $n_0^{1/2}$, consistent with the expected standard deviation for the Poisson distribution, $\bar{N}^{1/2}$ [22].

Because diffusion along the nanochannel (x direction) is essentially one-dimensional, it has proven relatively straightforward to obtain full analytical expressions for the low-frequency noise spectrum. This was done by extending the calculations of Berezhkovskii and Bezrukov [23] for biological channels to a one-dimensional domain including both a detection region and access channels. Radiative boundary conditions represented the coupling between the channel and the outside reservoir. While the full analytical form of the solution is too cumbersome to reproduce here [24], it was also shown that the power spectrum of the fluctuations is well described by the empirical form

$$S(f) = \frac{S_0}{1 + (f/f_0)^{3/2}}, \tag{3}$$

which interpolates between the exact low- and high-frequency limits. Here S_0 and f_0 are known constants that depend on D, $\bar{N}$ and the device geometry.

The predicted noise spectra were compared to experiments in which the redox cycling current $i(t)$ was measured as a function of time under steady-state redox cycling conditions. It was found that the theory provides good fits to the measured power spectra. Interestingly, however, quantitative discrepancies in the measured values of S_0 and f_0 were reported, suggesting a systematic error in the assumptions made in the theory; this is discussed further in the next section.

For more complex geometries such as nanopore arrays or nanocavities it is not always possible to derive an analytical description of the noise spectrum. In this case, simulations can be used to describe the electrochemical signals for arbitrary geometric sensor designs. While finite-element simulations are routinely used to predict the concentration distribution and average currents generated in electrochemical devices, they do not provide insight into the fluctuations of the signal. As a consequence, finite-difference and finite-element simulations are unsuitable for a description of the noise spectra. One approach to predict the current fluctuations in electrochemical sensors is given by random walk simulations that take into account the Brownian motion of the redox-active molecules. In such a simulation, the movement of individual molecules is modeled by discrete displacements in arbitrary but uniformly distributed directions within a discrete time-step [25, 26]. The temporal and spacial step width are connected by the diffusion equation. Electrochemical reactions of the molecules are taken into account via appropriate boundary conditions that depend on the applied electrode potential. The electrochemical currents including fluctuations are obtained by summing up the individual electron transfer events over a certain time window. An advantage of such simulations is that molecule- or material-specific effects like adsorption can be included in the model at a molecular level [27].

5.2 Electrochemical correlation spectroscopy

We argued above that the (low-frequency) power spectrum of the electrochemical current, $S(f)$, encodes information about the Brownian dynamics of molecules entering and leaving the detection region of a nanofluidic thin-layer cell. This is analogous to Fluorescence Correlation Spectroscopy (FCS), a technique in which the fluorescent signal from molecules diffusing in and out of a laser spot is used to study Brownian dynamics [28]. This has led us to coin the term Electrochemical Correlation Spectroscopy (ECS) to describe this approach [24,29]. Like FCS, ECS provides microscopic information about the Brownian motion of the molecules being detected.

The average redox cycling current takes the form $\bar{i} = \bar{N}i_0$ and fluctuations around this mean have a standard deviation determined by the Poisson distribution, $\delta i = \delta N i_0 = \bar{N}^{1/2} i_0$. These results hold for any value of i_0 so long as the molecules do not interact with each other. Combining these two equations in two unknowns therefore provides a way to extract values for $\bar{N}$ and i_0 based solely on measurements of $\bar{i}$ and δi, independent of any particular model for mass transport. This can then be compared to predictions such as $i_0 = z_e e D / h^2$ for purely diffusive mass transport.

Interestingly, and to our initial consternation, extracting $\bar{N}$ and i_0 from experimental data systematically yielded higher values of $\bar{N}$ and lower values of i_0 than would be expected from the known concentration/volume and diffusion coefficient/electrode spacing, respectively. While initially wrongly attributed to the idealized geometry used in the model [22], further experiments showed that the degree of discrepancy depended systematically on, e.g., the analyte concentration, the electrode potential and how the electrode surface was prepared. Since the value of i_0 depends only on the one unknown quantity D (z_e, e and h being fixed and known), this indicated that, contrary to commonly accepted assumptions in the electrochemistry community, mass transport could not be described in terms of simple bulk diffusion in these nanofluidic systems.

A second, related discrepancy emerged from a more detailed analysis of the electrochemical current power spectrum, $S(f)$. As indicated by Eq. (3), this spectrum exhibits white noise at low frequencies and crosses over to a diffusive $f^{-3/2}$ behavior at high frequencies. The crossover frequency, f_0, takes the form $f_0 = D\eta$, where η is a parameter that depends only on the (constant, known) geometry of the device [24]. Surprisingly, experiments indicate that f_0 is systematically lower than expected for pure diffusion as characterized by the bulk value of the diffusion coefficient D, once again indicating that D is effectively smaller in the nanodevices, typically by a factor 2–4 for outer-sphere systems.

The proposed solution to this apparent discrepancy is that electrochemically active molecules, even those of the prototypical outer sphere sort, undergo reversible, aspecific adsorption to the surface of electrodes, and that their diffusion is largely suppressed while they are adsorbed [21,30]. Diffusion in the nanochannels then consists of free Brownian motion interspersed with quasi-immobile periods on one of the available surfaces. This reconciles in a self-consistent, quantitative manner the observations of a smaller i_0 (electron shuttling is slower due to the time lost while adsorbed), a smaller f_0 (longitudinal diffusion is similarly hindered) and a larger $\bar{N}$ (the solution is still in diffusive equilibrium with a bulk reservoir and has the same bulk density, while in addition an excess of molecules are reversible adsorbed) [31]. This interpretation was further supported by studies of the transient response of the nanofluidic devices [32] as well as direct measurements of i_0 at the single-molecule level [33,34].

6 Single-molecule measurements

The ultimate limit of sensitivity for redox cycling is the detection of individual electrochemically active molecules as they generate a current between the two electrodes.

In thin-layer cells which are fully isolated from the environment, such as the tip-based systems in which a small volume of solution is trapped [18,19], the number of molecules N is fixed, as is in principle the average electrochemical current $\bar{i}$. Signatures of discreteness have however been reported. In the first report of single-molecule detection, in which wax-coated tips were used to create the cell [18], slow fluctuations were observed which were attributed to single molecules becoming trapped in the wax and subsequently released. In the subsequent work based on glass capillaries, stable currents were instead observed. But in this case the experimental system was additionally stable enough to allow repeated experiments in which new volumes of solution were trapped from a large reservoir [19]. The authors reported that the diffusion-limited current obtained at concentrations near $\bar{N} = 1$ differed substantially between successive runs. The observed values of the current appeared to vary in an approximately quantized manner, suggesting that different numbers of molecules N were trapped in the different experiments as per Eq. (2). Theoretically, one would expect the relative probability of obtaining different values of N to follow the Poisson distribution, $P_N = \bar{N}^N e^{-\bar{N}}/N!$ However, insufficient data using the same cell were available to test this quantitatively.

In thin-layer cells that are in contact with a bath, on the other hand, N is always free to fluctuate. $\bar{i} = \delta i$ when the concentration is so low that $\bar{N} = 1$, at which point the current signal becomes purely stochastic, increasing or decreasing by steps of i_0 each case that a molecule enters or leaves the detection region, respectively. Such measurements have been reported in both an organic solvent [33] and water [34]. While this could in principle allow obtaining extensive statistics on, e.g., the distribution of residence times under stationary conditions, allowing for a detailed comparison with theory, this has not proven possible so far in practice. This is due to the relationship between the residence times for the molecules inside the detection region of the device and the response time of existing measurement systems:

- A single-molecule event can be defined as starting when a molecule diffuses into the detection region and ending once the molecule exits this region. That is, the residence time is effectively the first-passage time for Brownian motion in a one-dimensional domain with absorbing boundary conditions [35]. The solution to this problem is well known [36]: the distribution of first-passage times diverges as $t^{-3/2}$ at short times (with a cutoff for times shorter than the z-direction transit time, below which the electrochemical signal is undefined) and falls off exponentially at long times.
- Measuring single-molecule currents $i_0 \simeq 10$ fA is near the limit of sensitivity of modern ammeters, and as a result the measured signals must be filtered substantially in the experiments. In practice this translates in response times on the order of tenths of a second. Consequently, only events that are of this duration or longer can be resolved. In particular, many short events in the $t^{-3/2}$ part of the residence time distribution cannot be resolved and effectively appear as low-amplitude noise in the measured signal [25]. Deconvolution of the filter response is also impractical due to additional noise from the electronics.

7 Shot-like noise

As mentioned previously, experimental measurements of very small fluctuations in the high-frequency regime remain challenging. Nevertheless, using random walk
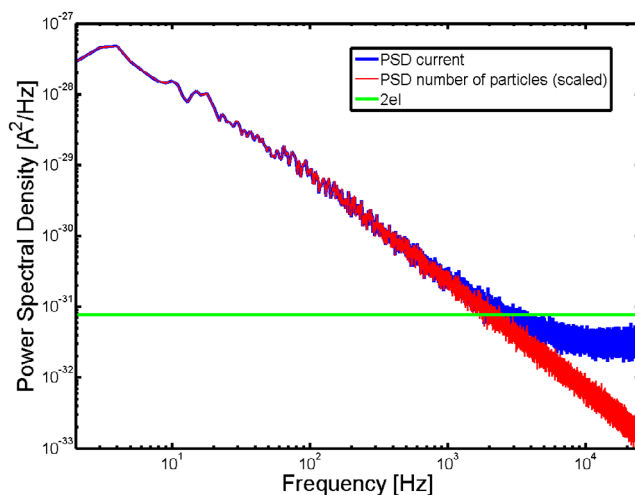
Fig. 4. Simulated power spectral density of a nanofluidic redox cycling sensor. The blue curve shows the total power spectral density of the sensor obtained from the simulated current. The red curve displays the scaled spectrum obtained by considering only the fluctuation of the number of particles inside the active region of the sensor. The green line indicates the theoretical shot noise level, $2e\bar{i}$.

simulations it is possible to predict noise spectra from electrochemical devices in operation over the whole frequency range. In Fig. 4, simulated noise spectra of a nanofluidic redox cycling sensor are shown. The blue curve depicts the power spectral density calculated from the simulated redox cycling current, $i(t)$. The red curve instead shows the power spectral density calculated from the number of molecules $N(t)$ inside the active volume of the nanofluidic sensor (that is, the domain enclosed by the two electrodes). The spectrum calculated from the number of molecules inside the active volume follows the diffusive $f^{-3/2}$ behavior described above. One could intuitively expect that the Brownian motion driving molecules from one electrode to the other should generate a white noise spectrum with the magnitude of classical shot noise $2e\bar{i}$. We see in Fig. 4 that the current spectrum, which includes the fluctuations associated with shuttling, indeed differs from the $f^{-3/2}$ decay after a transition frequency of approximately 2 kHz and evolves into a white-noise spectrum for higher frequencies, as expected. However, the magnitude of the shot-like noise is lower than predicted. This becomes evident by comparing the simulated trace with the theoretical shot noise, depicted by the green curve.

To further investigate only the shot-like noise, which is caused by the Brownian motion in between the electrodes and not by the low-frequency fluctuations of molecules in and out of the sensor's active area, we simulated a sensor geometry consisting of two infinite parallel plate electrodes. Here, the number of molecules participating in redox cycling stays constant and fluctuation noise is excluded. In Fig. 5, the noise spectra for three different electrode distances are shown. For low frequencies, all noise spectra feature a white-noise behavior with a magnitude lower than $2e\bar{i}$. Interestingly, there is an increase of the noise level to the expected $2e\bar{i}$ for higher frequencies after a transition regime. The ratio of the two white noise plateaus at high and low frequencies is approximately 3. As we can see explicitly by comparing the spectra for different inter-electrode distances h, the frequency of the transition regime corresponds to the inverse time it takes for a molecule to diffuse from one electrode to the other. This reflects the fact that electron-transfer events from each individual molecule are not
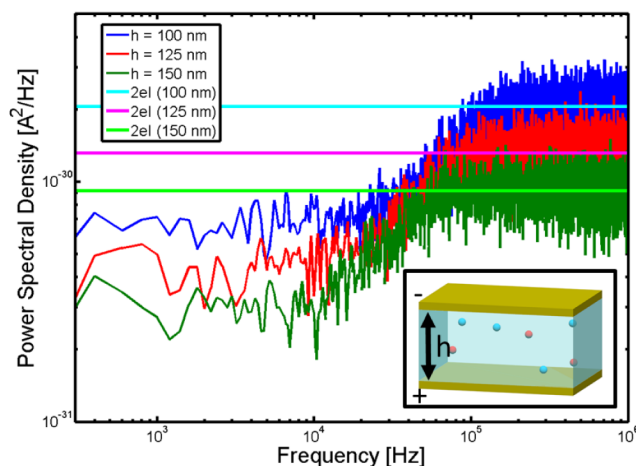
Fig. 5. Simulated redox cycling shot-like noise for two infinite parallel electrodes with different interelectrode spacings.

uncorrelated random events, since the molecule must travel back and forth across the gap during each cycle. To the best of our knowledge, the empirical simulation results presented here have not been elucidated analytically at this time.

8 Active transport

The active transport of particles in nanofluidic thin-layer cells by pressure-driven flow is desirable for practical analytical applications, i.e., for transporting analyte molecules to the electrode-pair detection area in the nanochannel. Driven flow leads to a bias on Brownian motion and to a corresponding shift in the power spectral density, and it is expected to considerably improve the sensitivity of single-molecule measurements [25].

A nanochannel exhibits a large hydraulic resitance due to its small cross section which opposes the generation of high flow rates. Experimentally, flow rates have been achieved which reduce the average (Brownian) traversal time of a particle through the nanochannel by about one order of magnitude [29,37]. At these low flow velocities, the solvent is driven entirely laminarily, and the flow does not affect Brownian transport in the high frequency shot noise regime. Thus, the separation of time scales of longitudinal transport along the channel and vertical shuttling caused by the very shallow aspect ratio of the device geometry also applies here.

The particle transport *along* the nanochannel at longer time scales can be described by a one-dimensional bias to the random walk. That is, while the solvent follows a Poiseuille flow, *vertical* diffusion takes place on such a short time scale that each molecule evenly samples all velocities of the vertical parabolic flow profile in the channel (this corresponds to surface Péclet numbers below unity at Reynolds numbers smaller than 0.001 [21]). Equivalent to an advection-diffusion equation, particle transport can be described by a one-dimensional Fokker-Planck equation, $\frac{\partial}{\partial t} f(x,t) = D \frac{\partial^2}{\partial x^2} f(x,t) - v \frac{\partial}{\partial x} f(x,t)$, where f is the number fluctuation correlation function [29]. The *effective* velocity of a particle is reduced by adsorption in the same way as its diffusivity: molecules do not advect while adsorbed and thus the average speed is reduced by the fraction of adsorption as compared to the solvent velocity.
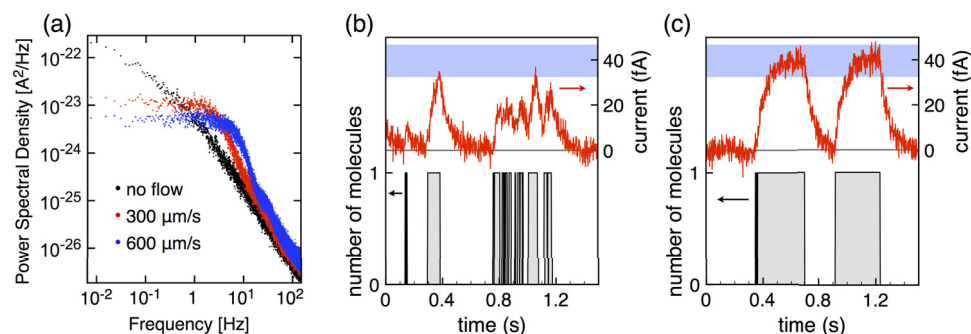
Fig. 6. One-dimensional random-walk simulations of active transport. (a) The PSD as a function of advection transport in a nanofluidic thin-layer cell (length $35\,\mu$m) is shown. Fast flow reduces the traversal time of particles between the electrode pair in the nanochannel, thus shifting the PSD of the detected current to higher frequencies. (b) Simulated molecule number (black) for diffusion only and corresponding current (red) after accounting for the measurement electronics. The blue band indicates the steady-state single-molecule current; most events are too short to reach this level. (c) Corresponding data in the presence of advective flow. Single-molecule events now have a well-defined duration and reach the expected current level. (b) and (c) reprinted with permission from ref. [3]. Copyright 2012 American Chemical Society.

Advection reduces the transit time of particles through the nanochannel and suppresses correlated events arising from particles diffusing back and forth across the edges of the detection region. The net effect for current correlation analysis is to shift the cutoff in the power spectral density to higher frequencies (see Fig. 6a) and we have previously used this shift for the determination of ultra-low flow rates [29]. Alternatively, in a more complex geometry two electrode pairs located downstream of each other were employed to detect the time-of-flight of number density fluctuations along the nanochannel. In this way, these Brownian fluctuations were used as a marker for liquid flow [29,37].

We expect that the combination of active transport and redox cycling will be most beneficial in future single-molecule measurements. As shown above, the slow instrumental reponse times in most sensitive current sensing excludes most single particles entering the detection area from being detected. If they move by a random walk exclusively, most particles do not traverse the nanochannel, but instead exit from the same end as they entered from shortly beforehand. Therefore, they do not occupy the volume between the electrodes long enough to generate a measureable redox current [25]. However, if molecules are advected fast enough to overcome their longitudinal diffusion, each of them will enter the nanochannel and traverse it in a (largely) controlled time span set by the liquid flow velocity. If this time is as long as the ∼100 ms of the instrumental response, than each single-molecule event will be detected reliably with a well defined event duration (see Fig. 6b).

Such a measurement has been analyzed numerically [25], but it has not been implemented experimentally yet.

9 Outlook

We have argued that miniaturized electrochemical devices represent an emerging class of experimental systems in which Brownian dynamics become manifest. This represents a hurdle for the downscaling of conventional sensor designs since the

corresponding current fluctuation sets new limits to the minimum amount of electrical noise that can be achieved. On the other hand it also creates opportunities for the study of fundamental processes and may yet lead to new types of sensors based on detecting mesoscopic or discrete amounts of molecules. Understanding the manifestations of Brownian motion and how they can be exploited represents the next important step in this process.

References

1. A.J. Bard, L.R. Faulkner, *Electrochemical methods - Fundamentals and Applications*, 2nd ed. (John Wiley & Sons, New York, 2001), p. 137
2. L. Rassaei, P.S. Singh, S.G. Lemay Anal. Chem. **2011**, 3974 (2011)
3. S.G. Lemay, S. Kang, K. Mathwig, P.S. Singh, Acc. Chem. Res. **46**, 369 (2013)
4. K.B. Oldham, J. Electroanal. Chem. **323**, 53 (1992)
5. V.A. Tyagai, Electrochim. Acta **16**, 1647 (1971)
6. G. Blanc, C. Gabrielli, M. Keddam, Electrochim. Acta **20**, 687 (1975)
7. G. Blanc, I. Epelboin, C. Gabrielli, M. Keedam, J. Electroanal. Chem. **75**, 97 (1977)
8. C. Gabrielli, F. Huet, M. Keddam, Electrochim. Acta **31**, 1025 (1986)
9. A. Hassibi, R. Navid, R.W. Dutton, T.H. Lee, J. Appl. Phys. **96**, 1074 (2004)
10. G. Mézáros, I. Szenes, B. Lengyel, Electrochem. Comm. **6**, 1185 (2004)
11. D. Krapf, Phys. Chem. Chem. Phys. **15**, 459 (2013)
12. O. Niwa, M. Morita, H. Tabei, Anal. Chem. **62**, 447 (1990)
13. E.D. Goluch, B. Wolfrum, P.S. Singh, M.A.G. Zevenbergen, S.G. Lemay, Anal. Bioanal. Chem. (**394**), 447 (2009)
14. G. Zhao, D.M. Giolando, J.R. Kirchhoff, Anal. Chem. **67**, 1491 (1995)
15. C.X. Ma, N.M. Contento, L.R. Gibson, P.W. Bohn, ACS Nano **7**, 5483 (2013)
16. C.X. Ma, N.M. Contento, L.R. Gibson, P.W. Bohn, Anal. Chem. **85**, 9882 (2013)
17. L.B. Anderson, C.N. Reilley, J. Electroanal. Chem. **10**, 538 (1965)
18. F.R.F. Fan, A.J. Bard, Science **267**, 871 (1995)
19. P. Sun, M.V. Mirkin, J. Am. Chem. Soc. **130**, 8241 (2008)
20. M.A.G. Zevenbergen, B.L. Wolfrum, E.D. Goluch, P.S. Singh, S.G. Lemay, J. Am. Chem. Soc. **131**, 11471 (2009)
21. K. Mathwig, S.G. Lemay, Electrochim. Acta **112**, 943 (2013)
22. M.A.G. Zevenbergen, D. Krapf, M.R. Zuiddam, S.G. Lemay, Nano Lett. **7**, 384 (2007)
23. S.M. Bezrukov, A.M. Berezhkovskii, M.A. Pustovoit, A. Szabo, J. Chem. Phys. **113**, 8206 (2000)
24. M.A.G. Zevenbergen, P.S. Singh, E.D. Goluch, B.L. Wolfrum, S.G. Lemay, Anal. Chem. **81**, 8203 (2009)
25. P.S. Singh, E. Kätelhön, K. Mathwig, B. Wolfrum, S.G. Lemay, ACS Nano **6**, 9662 (2012)
26. E. Kätelhön, K.J. Krause, P.S. Singh, S.G. Lemay, B. Wolfrum, J. Am. Chem. Soc. **135**, 8874 (2013)
27. E. Kätelhön, K.J. Krause, K. Mathwig, S.G. Lemay, B. Wolfrum, ACS Nano **8**, 4924 (2014)
28. D. Magde, E. Elson, W.W. Webb, Phys. Rev. Lett. **29**, 705 (1972)
29. K. Mathwig, D. Mampallil, S. Kang, S.G. Lemay, Phys. Rev. Lett. **109**, 118302 (2012)
30. D. Mampallil, K. Mathwig, S. Kang, S.G. Lemay, J. Phys. Chem. Lett. **5**, 636 (2014)
31. P.S. Singh, H.-S.M. Chan, S. Kang, S.G. Lemay, J. Am. Chem. Soc. **45**, 18289 (2011)

32. S. Kang, K. Mathwig, S.G. Lemay, Lab Chip **12**, 1262 (2012)
33. M.A.G. Zevenbergen, P.S. Singh, E.D. Goluch, B.L. Wolfrum, S.G. Lemay, Nano Lett. **11**, 2881 (2011)
34. S. Kang, A.F. Nieuwenhuis, K. Mathwig, D. Mampallil, S.G. Lemay, ACS Nano **7**, 10931 (2013)
35. W. Fellner, *An Introduction to Probability Theory and Its Application*, 3rd edn. (Wiley, New York, 1968)
36. S. Redner, *A Guide to First-Passage Processes* (Cambridge University Press, Cambridge, 2001)
37. K. Mathwig, S.G. Lemay, Micromachines **4**, 138 (2013)